

Mathematical Modelling of Different Types of Body Support Surface for Pressure Ulcer Prevention

Mahbub C. Mishu, Venketesh N. Dubey, Tamas Hickish, Jonathan Cole

Abstract—Pressure ulcer is a common problem for today's healthcare industry. It occurs due to external load applied to the skin. Also when the subject is immobile for a longer period of time and there is continuous load applied to a particular area of human body, blood flow gets reduced and as a result pressure ulcer develops. Body support surface has a significant role in preventing ulceration so it is important to know the characteristics of support surface under loading conditions. In this paper we have presented mathematical models of different types of viscoelastic materials and also we have shown the validation of our simulation results with experiments.

Keywords—Pressure ulcer, viscoelastic material, mathematical model, experimental validation.

I. INTRODUCTION

THE healthcare industry is facing a major challenge against pressure ulcers in hospitals. Due to this, a major expenditure is spent within the industry each year. In UK, research shows that each year approximately 412,000 people develop pressure ulcers [1] in hospitals while they are lying on beds or sitting on chair for long periods. This costs the UK hospitals approximately £1.4-£2.1 billion a year (nearly 4% of NHS budget) [1], [2]. People with mobility impairments, spinal cord injury, head trauma or multiple sclerosis are the main victim of pressure ulcer [3], [4]. Also, people in comas or people in long surgical procedure develop pressure ulcers [5]. These figures indicate the significance of preventing pressure ulcer in healthcare industry.

II. PRESSURE ULCER FORMATION

Pressure ulcer is confined to a small area of tissue breakdown in skin [6]. It occurs in a situation when people are immobile and subjected to prolonged mechanical loads. Due to this loading, blood flow and the oxygen supply become insufficient to the soft tissues [2], [3] and that leads to Tissue Necrosis [3], [4]. In early stages, it is known as pressure sore/decubitus ulcer/ ischemic ulcer or bedsore, and later, it leads to ulceration. Current studies suggest a pressure higher than 32 mm Hg [3], [4] applied to a skin can be sufficient to cause pressure sore, if the patient is immobile for two hours. The interface pressure between the skin and the supporting surface (e.g. mattresses, chairs, cushions etc.) is an important

Mahbub C Mishu, PhD researcher, Faculty of Science and Technology, Bournemouth University, UK. (e-mail: mmishu@bournemouth.ac.uk).

Venketesh N. Dubey, Associate Professor, Faculty of Science and Technology, Bournemouth University, UK. (e-mail:vdubey@bournemouth.ac.uk).

Tamas Hickish MD Poole Hospital, Visiting Professor Bournemouth University, UK. (e-mail:tamas.hickish@rbch.nhs.uk).

Jonathan Cole, DM, Poole Hospital, Visiting Professor, Bournemouth University, UK. (e-mail:jonathan.cole@poole.nhs.uk).

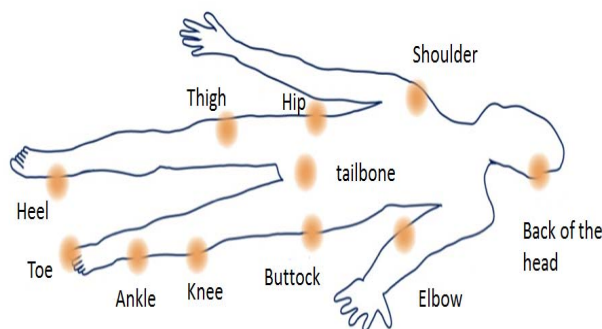


Fig. 1. Common pressure points where ulceration can occur [8]

parameter to consider. If the pressure value is higher than 32 mmHg, then it is considered as a risk of developing ischemia. Studies also [7], show that in terms of susceptibility to mechanical loading, the muscle tissues are more susceptible in comparison to skin. Fig. 1 shows common pressure points in human body. According to the European Pressure Ulcer Advisory Panel (EPUAP) [9], pressure ulcer can be classified in four different stages.

- Stage 1: Non-blanchable erythema refers the intact skin with non-blanchable redness of a localized area usually over a bony prominence. The reddened area remains red after the pressure is relieved. The area may be painful, firm and warmer as compared to adjacent tissue.
- Stage 2: Partial Thickness, in this stage a shallow open red pink ulcer is visible due to the partial thickness loss of the dermis. It can also be represented as an open serum-filled/sero-sanguinous filled blister. A shiny/ dry shallow ulcer results without any slough or bruising.
- Stage 3: Full thickness skin Loss: In this stage ulcer gets worse with full thickness skin loss and due to this the tissue necrosis results in a patients body but not through bone tendon or joint capsule.
- Stage 4: Full thickness tissue loss: Ulcer reaches to the bone, tendon or muscle. The depth of Stage 4 pressure ulcers varies by anatomical location. Stage 4 ulcers can extend into muscle and/or supporting structures (e.g., fascia, tendon or joint capsule) making osteomyelitis or osteitis likely to occur.

Fig. 2 shows different stages of pressure ulcers in living tissues.

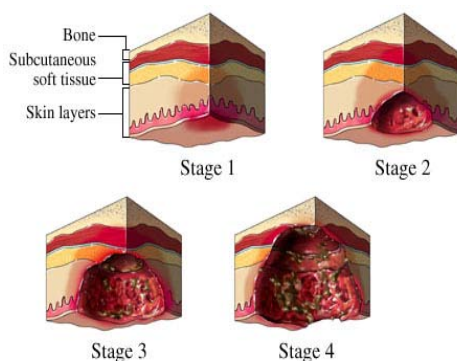


Fig. 2. Different stages of pressure ulcers according to EPUAP [9]

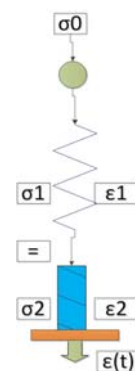


Fig. 3. Maxwell model (spring in series with dashpot) [12]

III. SUPPORT SURFACE MODELLING

In order to characterize the support surface mathematically, initially we considered three theoretical models; Maxwell model, Kelvin-Voigt model and Maxwell Wiechert model. All these models are different combination of spring and dashpot. We observe the output response of these models due to applied load and finally we have developed a new model for surface. Viscoelastic material usually provides a special type of behaviour which is a combination of viscous and elastic responses. Thus the word viscoelastic is formed. The elastic response comes from spring and the viscous behaviour comes from the dashpot. Viscous response means, when load is applied to the material, it deforms gradually with respect to time and when load is removed, it starts coming back to its original shape. On the other hand, elastic response is quite rapid during loading and unloading situations. From the theoretical stand point, we know viscoelastic materials have a tendency to start deforming gradually when load is applied to the surface and when load is removed, it starts getting back to its original position (relaxation of material) [10], [11]. To establish this we have developed support surface model and validated with experimental results.

A. Maxwell Model

In Maxwell model, a spring and dash-pot is placed in series (shown in Fig. 3). Stress in Maxwell model is same for both spring and dashpot. The deformation of this type of model can be obtained by dividing the total strain into one for the spring and one for the dash-pot. Following mathematical equations describe the deformation in Maxwell model.

$$\varepsilon_1(t) = \frac{1}{E}\sigma(t) \quad (1)$$

$$\varepsilon_2(t) = \frac{1}{\eta} \frac{d\varepsilon}{dt} \quad (2)$$

Equation 1 describes the deformation in spring and equation 2 describes that for the dashpot part. The total deformation of the model is described by equation 3.

$$\varepsilon(t) = \varepsilon_1(t) + \varepsilon_2(t) \quad (3)$$

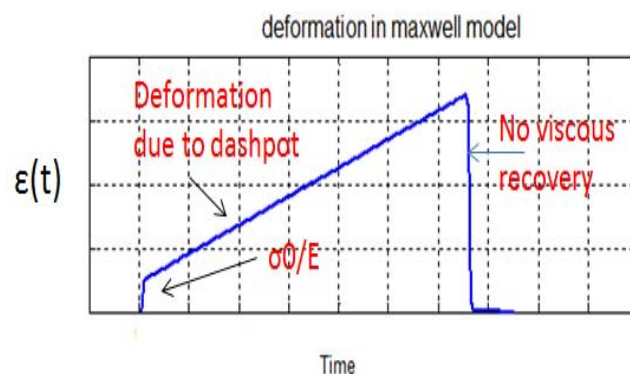


Fig. 4. Deformation and relaxation behaviour in Maxwell model

Where $\varepsilon(t)$ is total deformation, $\varepsilon_1(t)$ is deformation due to spring, $\varepsilon_2(t)$ is deformation due to dashpot, E is the materials Youngs modulus, η is viscosity of material, t is time of loading.

When initial stress (force/area) σ_0 is applied to the model it starts deforming. Also when the Maxwell model is subjected to a stress, the spring starts stretching instantly and dashpot takes time to react. So initial deformation of the material is $\varepsilon(0) = \frac{\sigma_0}{E}$. Due to initial deformation, the total deformation of Maxwell model can be described as

$$\varepsilon(t) = \sigma_0 \left(\frac{1}{\eta}t + \frac{1}{E} \right) \quad (4)$$

When the load is removed, the spring again reacts instantly. Hence there is an instant elastic recovery (due to spring) $\frac{\sigma_0}{E}$. The full deformation and recovery behaviour as modelled is shown in Fig. 4. Although Maxwell model shows deformation, but it does not provide any viscous recovery behaviour when load is removed. The response from this type of model is elastic.

B. Kelvin-Voigt Model

Kelvin-Voigt model consists of a spring and a dashpot in parallel (shown in Fig. 5). In this type of model, deformation in spring and dashpot are same but stresses are different. Also this type of model establishes better deformation results compared

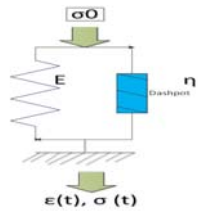


Fig. 5. Kelvin-Voigt model (spring and dashpot in parallel)[12]

to Maxwell model. Mathematical equations which describe relaxation and deformation of Kelvin-Voigt model are given below:

$$\sigma(t) = E\varepsilon(t) + \eta \frac{d\varepsilon}{dt} \quad (5)$$

$$\varepsilon(t) = \frac{\sigma_0}{E} - \frac{\eta}{E} \frac{d\varepsilon}{dt} \quad (6)$$

Where $\sigma(t)$ is relaxation of stress, $\varepsilon(t)$ is deformation of material, E is Young's modulus, η is viscosity (constant for soft foam), σ_0 is initial stress applied to the model and t is time.

When initial stress, σ_0 is applied to the model, spring will stretch due to its elastic nature, but is held back by the dash-pot. Since the spring does not change length, the stress is initially taken up by the dash-pot. The deformation thus starts with an initial slope $\frac{\sigma_0}{\eta}$. Deformation then occurs and some of the stress is transferred from the dash-pot to the spring. The slope of the deformation curve becomes $\frac{\sigma_2}{\eta}$ where σ_2 is the stress in the dashpot. In the limit when $\sigma_2=0$, the spring takes all the stress and maximum deformation becomes $\frac{\sigma_0}{E}$. By solving the first order non-homogeneous differential equation (5) with an initial condition $\varepsilon(0) = 0$ provides the following equation for deformation of Kelvin-Voigt model.

$$\varepsilon(t) = \frac{\sigma_0}{E} (1 - e^{-\frac{E}{\eta}t}) \quad (7)$$

Thus deformation function becomes,

$$\delta(t) = \frac{1}{E} (1 - e^{-\frac{t}{t_R}}) \quad (8)$$

Where $t_R = \frac{\eta}{E}$. The variable t_R , is called retardation time of the material. It is a measure of the time taken for the deformation to occur. If the retardation time is shorter, deformation occurs more rapidly. When the initial stress is removed in Kelvin model, spring respond instantly but dashpot holds it back. The spring however eventually pulls the dash-pot back to its original zero position in a given time and thus full recovery occurs. Deformation and relaxation from Kelvin-Voigt as modelled is shown in Fig. 6.

The Kelvin-Voigt Model is ideal to optimize the deformation behaviour but it does not provide a total viscous relaxation. This type of model returns elastic retardation when the initial stress is removed.

C. Maxwell-Wiechert Model

Maxwell model and Kelvin-Voigt model does not provide full viscoelastic behaviour. In Maxwell model, the deformation takes place linearly and in Kelvin-Voigt model, although the

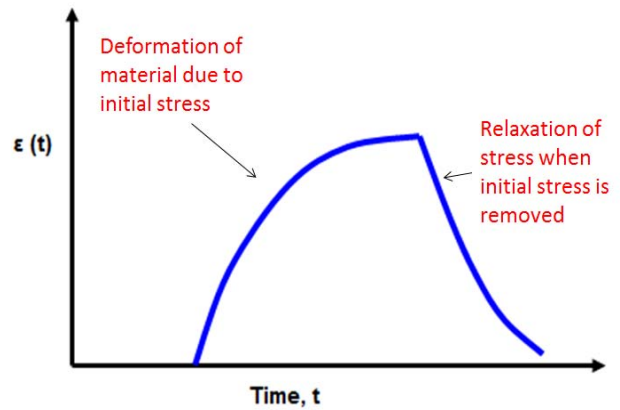


Fig. 6. Deformation and relaxation in kelvin-voigt model

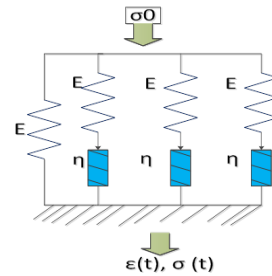


Fig. 7. Maxwell-Wiechert model[12]

deformation is nonlinear, the recovery or relaxation of stress is not viscous. Maxwell-Wiechert model is considered where three single Maxwell block is connected in parallel to a single spring. This model is also known as generalized Maxwell model (shown in Fig. 7). The Maxwell-Wiechert model consists of three different Maxwell units in parallel. In order to observe soft material behaviour, material parameter is set same for all three blocks. By simulating this model, deformation and relaxation behaviour of soft material is obtained. Mathematical equation which describes viscous characteristics of this model are given below

$$\varepsilon(t) = \frac{\sigma_0}{E} + \frac{\sigma_0}{\eta}t + \frac{\sigma_0}{\eta}t + \frac{\sigma_0}{\eta}t + \frac{\sigma_0}{E}(1 - e^{-\frac{E}{\eta}t}) \quad (9)$$

$\varepsilon(t)$ is deformation of material, σ_0 is initial stress applied to the material, E is Young's modulus of the material, η is the viscosity and t is time. In order to obtain relaxation behaviour following equation is used

$$\sigma(t) = \sigma_1(t) + \sigma_2(t) + \sigma_3(t) \quad (10)$$

where $\sigma_1(t) = \sigma_0 \cdot e^{-\frac{t}{t_1}}$, $\sigma_2(t) = \sigma_0 \cdot e^{-\frac{t}{t_2}}$ and $\sigma_3(t) = \sigma_0 \cdot e^{-\frac{t}{t_3}}$.

In Maxwell-Wiechert model, the deformation behaviour is viscoelastic but relaxation behaviour obtained from this model does not show a complete relaxation of stress and also it does not fully relaxed though the initial stress is removed completely. Fig. 8 shows the deformation and relaxation of stress by maxwell-wiechert model as developed:

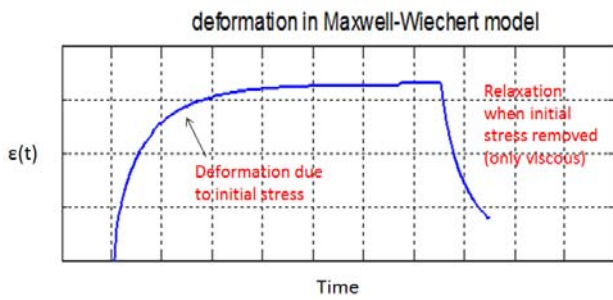


Fig. 8. Deformation and relaxation in Maxwell-Wiechert model

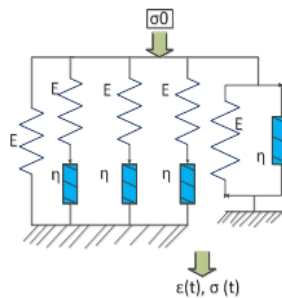


Fig. 9. Developed new model

D. An Enhanced Model to Characterize Support Surface Behaviour

Fig. (4, 6 and 8) shows the output response of three theoretical models and none of the model shows complete viscoelastic behaviour due to external load as could be representative in pressure ulcer formation point of view. So we have developed a support surface model which may ensure materials viscoelastic behaviour in pressure sore formation. Also the deformation and relaxation obtained by this enhanced model are purely viscoelastic. Fig. 9 shows our developed model to characterize soft materials viscoelastic behaviour. The model is mathematically described by following equation and shown in Fig. 9.

$$\varepsilon(t) = \frac{\sigma_0}{E} + \sum_{n=0}^3 \frac{\sigma_n}{\eta} t + \frac{\sigma_0}{E} (1 - e^{-\frac{E}{\eta} t}) + \frac{\sigma_0}{E} - \frac{\eta}{E} \frac{d\varepsilon}{dt} \quad (11)$$

The model shown comprises of Maxwell-Wiechert block connected to a Kelvin-Voigt block. In order to validate this model, experiments are conducted and discussed simulation results are obtained to show good viscoelastic deformation and relaxation behaviour both. Fig. 10 shows a deformation graph from the model (developed).

To visualize the response from all different types of models, we developed a custom made graphic user interface (GUI) in MATLAB where we applied load to all different models and the GUI shows us the response developed. Fig. 11 shows the user interface.

In order to begin simulation of different models, first material parameters are estimated. These estimations are obtained from a literature search and taken from previous

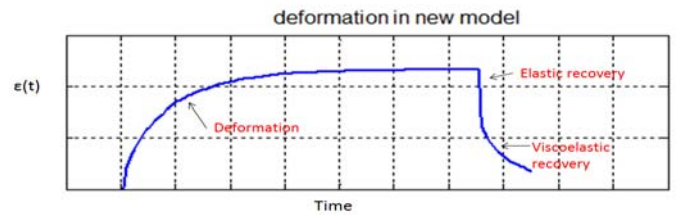


Fig. 10. viscoelastic behaviour of developed new model (obtain from simulation)

research on materials. Table I shows the estimation of parameters for simulation of models.

TABLE I
 PARAMETER ESTIMATION FOR SIMULATION [13], [14], [15], [16]

Model name	Young's modulus in MPa
Maxwell	0.025-0.0360
Kelvin-Voigt	0.025-0.0360
Maxwell-Wiechert	0.025-0.0360
Developed model	0.025-0.0360

IV. EXPERIMENTAL SETUP AND VALIDATION OF SIMULATION

In order to conduct experiments, a mechanical indenter is used. Purpose of using such an indenter is to apply load more accurately. A circular wooden disc is placed at the top of the device so that load can be applied on a specified area. To get accurate data from the sensor, area of the indenter is chosen same as the area of the sensor. During the experiments force-sensing resistor (FSR) is used to measure the force which can be converted into pressure. This setup has a digital height gauge. Digital height gauge is used to measure the change in length of the indenter due to applied load. This change in length is used to find the Youngs modulus of material experimentally. Load is applied at the top of the indenter (wooden disc) and the height gauge measures the indenter displacement. Initial length of the indenter is measured as 0.3 m (without any material). The area of the indenter remains same as area of the sensor which is measured as 0.00000631 m². The weight of indenter is also taken into consideration. Fig. 12 shows the experimental setup for different types of materials.

From the experiment, we found viscous response from different materials and results obtained from experiment matched with the simulation result. When the load was applied into the material, it starts deforming gradually and the force sensor gets the force value. Fig. 13 shows experimental graph obtain in comparison to simulation results.

Recovery state (due to load removal) was not obtained during experiments because force sensor system we cannot get any value when there is no contact between the indenter tip and sensor. Thats why we have only shown the deformation during loading. This is the limitation of the current experiments.

V. CONCLUSION

In this paper, we have shown modelling of different types of viscoelastic material (used as body support surface). Also we

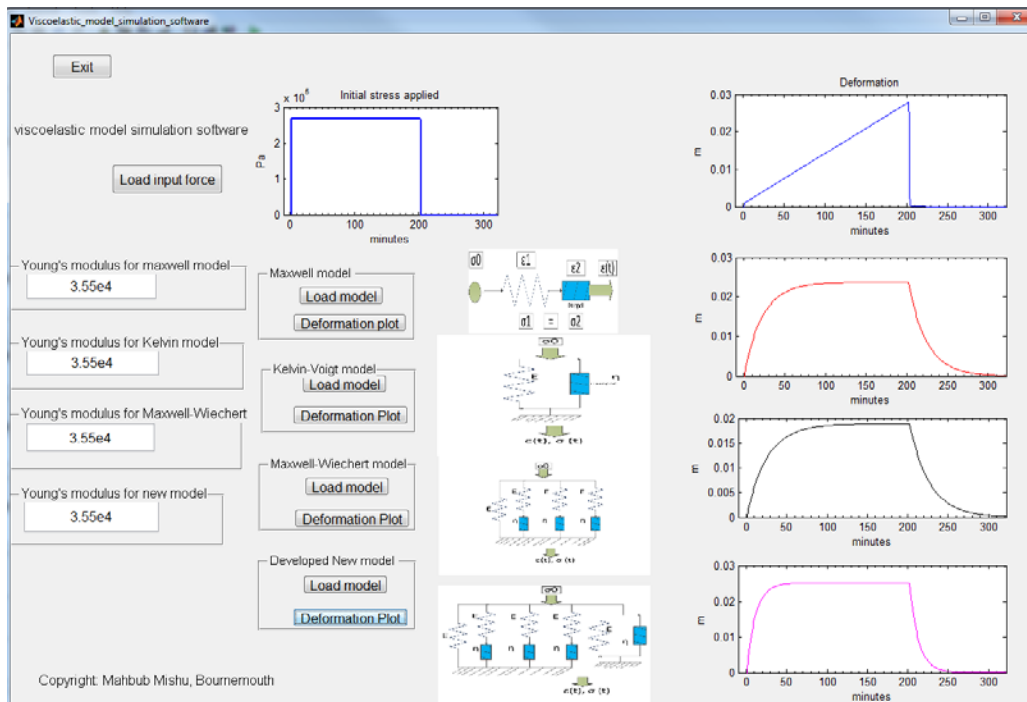


Fig. 11. Developed user interface in MATLAB



Fig. 12. experimental setup for different types of materials

have shown our developed model provides the closest match for support surfaces compared to three theoretical models. We also have shown the validation of our developed model through an experiment. These types of modelling and developments have significant importance for characterising support surface material for pressure ulcer prevention. To prevent ulceration in human body, we need to select the material (support surface) correctly. To cover a wide range of materials we developed a graphic user interface where materials characteristics can be seen and support surface could be designed. The main objective was to validate our developed model for variety of support surfaces.

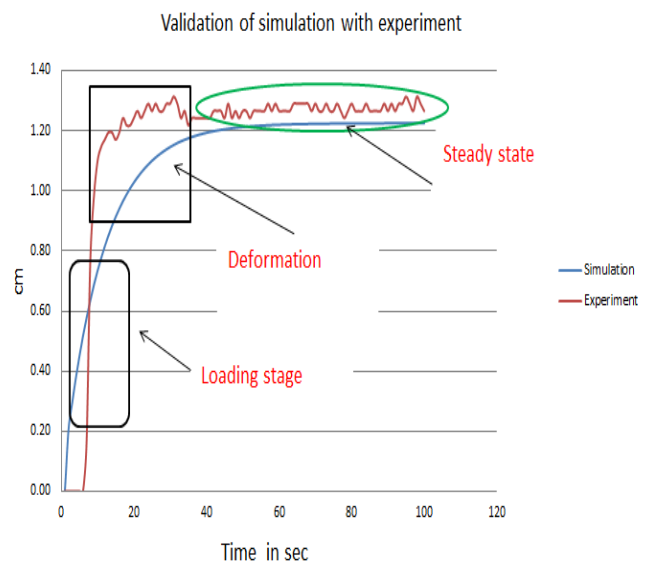


Fig. 13. experimental data along with simulation data

REFERENCES

- [1] G. Bennett, C. Dealey, and J. Posnett, "The cost of pressure ulcers in the uk," *Age and ageing*, vol. 33, no. 3, pp. 230–235, 2004.
- [2] C. Hsia, K. Liou, A. Aung, V. Foo, W. Huang, and J. Biswas, "Analysis and comparison of sleeping posture classification methods using pressure sensitive bed system," in *Engineering in Medicine and Biology Society, 2009. EMBC 2009. Annual International Conference of the IEEE. IEEE*, 2009, pp. 6131–6134.
- [3] A. Manohar and D. Bhatia, "Pressure detection and wireless interface for patient bed," in *Biomedical Circuits and Systems Conference, 2008. BioCAS 2008. IEEE. IEEE*, 2008, pp. 389–392.

- [4] L. R. Solis, A. Liggins, R. R. Uwiera, N. Poppe, E. Pehowich, P. Seres, R. B. Thompson, and V. K. Mushahwar, "Distribution of internal pressure around bony prominences: implications to deep tissue injury and effectiveness of intermittent electrical stimulation," *Annals of biomedical engineering*, vol. 40, no. 8, pp. 1740–1759, 2012.
- [5] N. Graves, F. Birrell, and M. Whitby, "Effect of pressure ulcers on length of hospital stay," *Infection Control and Hospital Epidemiology*, vol. 26, no. 3, pp. 293–297, 2005.
- [6] C. V. Bouten, C. W. Oomens, F. P. Baaijens, and D. L. Bader, "The etiology of pressure ulcers: skin deep or muscle bound?" *Archives of physical medicine and rehabilitation*, vol. 84, no. 4, pp. 616–619, 2003.
- [7] R. K. Daniel, D. L. Priest, and D. C. Wheatley, "Etiologic factors in pressure sores: an experimental model." *Archives of physical medicine and rehabilitation*, vol. 62, no. 10, pp. 492–498, 1981.
- [8] S. Saha, M. B. Smith, A. Totten, R. Fu, N. Wasson, B. Rahman, M. Motuapuaka, D. H. Hickam *et al.*, "Pressure ulcer treatment strategies: Comparative effectiveness," 2013.
- [9] Online, <http://www.spinal-injury.net/pressure-sore-stages-sci.htm>, accessed on 13.03.2014.
- [10] D. Roylance, "Engineering viscoelasticity," *Department of Materials Science and Engineering–Massachusetts Institute of Technology, Cambridge MA*, vol. 2139, pp. 1–37, 2001.
- [11] O. Weckner and N. A. Nik Mohamed, "Viscoelastic material models in peridynamics," *Applied Mathematics and Computation*, vol. 219, no. 11, pp. 6039–6043, 2013.
- [12] R. M. Christensen and L. Freund, "Theory of viscoelasticity," 1971.
- [13] L. Lundell, "Estimation of material functions using system identification techniques," 2012.
- [14] L. Hillström, M. Mossberg, and B. Lundberg, "Identification of complex modulus from measured strains on an axially impacted bar using least squares," *Journal of Sound and Vibration*, vol. 230, no. 3, pp. 689–707, 2000.
- [15] E. Zhang, J.-d. Chazot, J. Antoni *et al.*, "Parametric identification of elastic modulus of polymeric material in laminated glasses," in *System Identification*, vol. 16, no. 1, 2012, pp. 422–427.
- [16] S. Choi, S. W. Cha, and B. H. Oh, "Identification of viscoelastic behavior for early-age concrete based on measured strain and stress histories," *Materials and structures*, vol. 43, no. 8, pp. 1161–1175, 2010.